Journal of Applied Polymer Science

Antimicrobial Activity and Biodegradation Behavior of Poly(butylene adipate-*co*-terephthalate)/Clay Nanocomposites

Dibyendu Mondal,[1] Biplab Bhowmick,[1] Md. Masud R. Mollick,[1] Dipanwita Maity,[1] Nayan Ranjan Saha,[1] Vivek Rangarajan,[2] Dipak Rana,[3] Ramkrishna Sen,[2] Dipankar Chattopadhyay[1]

[1]Department of Polymer Science and Technology, University of Calcutta, Kolkata 700009, West Bengal, India

[2]Department of Biotechnology, Indian Institute of Technology Kharagpur, Kharagpur 721302, West Bengal, India

[3]Department of Chemical and Biological Engineering, Industrial Membrane Research Institute, University of Ottawa, Ottawa, Ontario K1N 6N5, Canada

Correspondence to: D. Chattopadhyay (E-mail: dipankar.chattopadhyay@gmail.com)

ABSTRACT: Poly(butylene adipate-*co*-terephthalate) (PBAT) nanocomposites films are prepared by a solution intercalation process using natural montmorillonite (MMT) and cetyltrimethylammonium bromide (CTAB)-modified montmorillonite (CMMT). Cation exchange technique has been used for modification of MMT by CTAB and characterized by Fourier transform infrared analysis, thermo-gravimetric analysis, and X-ray diffraction (XRD) studies. CMMT gives better dispersion in the PBAT matrix than MMT and is confirmed by XRD and transmission electron microscopy. Because of better compatibility of CMMT, water vapor transmission rate of PBAT decreases more in the presence of CMMT than MMT. The biodegradability of PBAT and its nanocomposite films are studied in compost and from the morphological analysis it is apparent that the PBAT/CMMT shows a lower biodegradation rate in comparison to the PBAT/MMT. The antimicrobial activity of PBAT and its nanocomposite films is tested by an inhibition zone method. Because of the presence of the quaternary ammonium group of CTAB-modified MMT, PBAT/CMMT nanocomposites show adequate antimicrobial activity. © 2013 Wiley Periodicals, Inc. J. Appl. Polym. Sci. **2014**, *131*, 40079.

KEYWORDS: biodegradable; clay; morphology; films

Received 15 July 2013; accepted 14 October 2013
DOI: 10.1002/app.40079

INTRODUCTION

Material scientists have shown huge interest in the field of nanocomposites comprising of biodegradable polymers and layered silicates due to their attracting mechanical properties,[1,2] improved water resistance properties,[3,4] lower water vapor permeability,[5] and enhanced thermal properties.[6] Ray et al.[7] observed remarkable improvement of materials properties of polylactide (PLA)/layered silicate nanocomposites in both the solid and melt states compare to the virgin PLA matrix. Considerable enhancement in thermal and mechanical properties along with significant biodegradability under controlled conditions in enzyme, pure microorganism (fungi), compost, and alkaline buffer solution of poly(ε-caprolactone)/layered silicate nanohybrids was studied by Singh et al.[8] In another work, Sancha et al.[9] investigated the permeability of Poly(vinyl alcohol) (PVA)-graft acrylonitrile/clay nanocomposites towards vapor and liquid molecules. Phua et al.[10] studied the biodegradation of poly(butylene succinate)/organo montmorillonite nanocomposites under controlled compost soil conditions.

The sodium montmorillonite (MMT) type of layer silicates clay is an octahedral alumina sheet sandwiched between two tetrahedral silica sheets.[11] Sodium montmorillonite, a hydrophilic clay, can be organically modified by introducing a long alkyl chain in the gallery gap via the cation-exchange process[12] to make the clay hydrophobic in nature as well as to increase its compatibility with organic polymers.

Poly(butylene adipate-*co*-terephthalate) (PBAT), trade name Ecovio, is an aliphatic–aromatic copolyester based on the monomers 1,4-butanediol, adipic acid, and terephthalic acid. It is a fully biodegradable polymer[13] and is resistant to water showing potential in its application for packaging films, compost bags and agricultural films.[14] Chen et al.[15] studied the thermal and mechano-chemical properties of PBAT/octadecylamine-modified montmorillonite nanocomposites while Mohanty and Nayak[16] illustrated the property enhancement of PBAT nanocomposites prepared by a melt blending technique using MMT, Cloisite 20A, Cloisite 30B, and Bentonite (B109) nanoclays.

The antimicrobial property of such nanocomposites makes it a versatile material in packaging applications. In this regard, Rhim et al.[17] reported that the nanocomposite films containing certain organically modified nanoclay offers strong

antimicrobial function against both Gram-positive and Gram-negative bacteria. They postulated that the quaternary ammonium groups present in the organically modified clays are responsible for the antimicrobial function of nanocomposite films.[18] These nanocomposite films with enhanced mechanical and gas barrier properties have a high potential for being used as food packaging materials.

In this article, we report the successful modification of MMT using CTAB and characterized using XRD, thermo-gravimetric analysis (TGA), and Fourier transform infrared analysis (FTIR). We have also formulated the nanocomposites of PBAT with unmodified and organically modified MMT using a solution intercalation process. The morphology of nanocomposites is investigated by X-ray diffraction (XRD) and transmission electron microscopy (TEM) analysis whereas scanning electron microscopy (SEM) is used to examine the surface morphology of biodegraded nanocomposite films. Biodegradability of nanocomposite films is calculated by measuring weight loss in compost. Furthermore, we have also studied water vapor transmission rates and the antimicrobial activity of PBAT nanocomposite films.

EXPERIMENTAL

Materials

PBAT (Ecovio) was purchased from baden aniline and soda factory (BASF). Unmodified montmorillonite clay (MMT) was obtained from Nanocor, USA with a cation-exchange capacity of 100 mequiv/100 g. Cetyl trimethylammonium bromide (CTAB) and chloroform were obtained from Merch (India).

Preparation of CTAB-Modified MMT

Organically modified MMT clay was prepared through a cation-exchange process which is as follows. MMT (2.0 g) was dispersed in 400 mL distilled water with vigorous mechanical stirring for 24 h at room temperature to prepare a uniformly suspended solution. An aqueous solution of CTAB was added drop wise to the suspended solution of MMT and was stirred vigorously at 80°C overnight to carry out the exchange of Na^+ of MMT by quaternary ammonium cation. To complete the modification of MMT in this process, we have adjusted the amount of CTAB equivalent to 100% of cation exchange capacity of MMT. The suspended organoclay was then filtered and washed repeatedly with distilled water until no AgBr precipitate was found by titrating the filtrate against 0.1*N* $AgNO_3$ solutions. Then organoclay was vacuum dried at 60°C for 24 h.

Preparation of PBAT/Clay Nanocomposites

Both the PBAT/MMT and PBAT/CTAB-modified montmorillonite (CMMT) nanocomposites were prepared using a solvent intercalation process. PBAT (2 g) was dissolved in 15 mL of chloroform at room temperature. The required amount of MMT and CMMT was dispersed in 10 mL of chloroform for 24 h and then each of the clay suspensions was sonicated for 30 min. PBAT/clay nanocomposites containing various wt % (2 wt %, 4 wt %, and 8 wt %) of each were produced by cautiously adding clay suspension into the PBAT solution with continuous stirring for 24 h, then the resultant solution was poured onto a glass plate at room temperature to make the thin nanocomposite films of uniform thickness. Thin films were obtained after the evaporation of solvent. Then films were dried at 60°C in a vacuum oven for 24 h to remove the residual solvent.

Material Characterization

XRD Analysis. XRD analysis of the nanocomposite samples was performed at room temperature by an X-PERT-PRO Panalytical diffractometer using Cu Kα ($\lambda = 1.5406$) as X-ray source at a generator voltage of 40 kV and current of 30 mA. The scanning rate was 1°/min. From the XRD data, the interlayer spacing of clay platelets was calculated using Bragg's law as follows:

$$d = \frac{\lambda}{2\mathrm{Sin}\,\theta}, \quad (1)$$

where d is d-spacing (nm), λ is wavelength of X-ray beam (nm), and θ is the angle of incidence.

Thermal Analysis. Thermogravimetric analyses of unmodified and organically modified clay were performed on a Mettler-Toledo TGA/SDTA 851 thermal analyzer in a dynamic atmosphere of nitrogen (flow rate = 30 cm^3/min). The samples were heated in a alumina crucible at a rate of 10°C/min over a temperature range of 30–500°C.

Fourier Transform Infrared Spectroscopy. FTIR spectroscopy experiments were performed with a Bruker-Optics Alpha-T spectrophotometer over the range 400–4000 cm^{-1}.

Scanning Electron Microscopy. To investigate the nature of surface degradation, the morphology of the films was examined under ZEISS, EVO 18 scanning electron microscope (SEM). For SEM analysis, biodegraded films were coated with gold in a sputter coater and observed under SEM at an accelerating voltage 15 kV.

Transmission Electron Microscopy. The nano-scale morphology of the PBAT/4 wt % MMT and PBAT/4 wt % CMMT nanocomposites was observed using TEM. TEM was performed on a high-resolution TEM (model: JEM 2010 EM) at 120 kV accelerating voltage.

Water Vapor Transmission Rate

Water vapor permeability of the layer silicate nanocomposite films was calculated in accordance with the modified ASTM E96-00 method.[19] Film samples were sealed over a 60 mm circular opening of a permeation cell containing calcium chloride (0% RH inside the cell). The permeation cells were then placed inside a desiccator containing the saturated sodium chloride solution (75% RH outside the cell), to create a 75% RH gradient across the film.[20] The water vapor permeability was determined from the weight gain of the permeation cell every 24 h until a constant rate of weight gain was attained. The water vapor transmission rate was calculated using the following equation[21]:

$$Q = \frac{WL}{S}, \quad (2)$$

where W is the increase in the desiccant weight per 24 h, L is the film thickness (cm), S is the exposed surface area (cm^2), and Q is the water vapor transmission rate (g/cm^2 per 24 h).

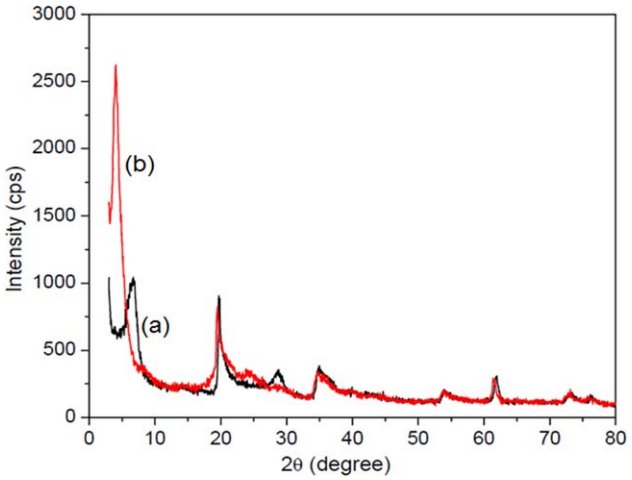

Figure 1. XRD patterns of (a) MMT and (b) CMMT. [Color figure can be viewed in the online issue, which is available at wileyonlinelibrary.com.]

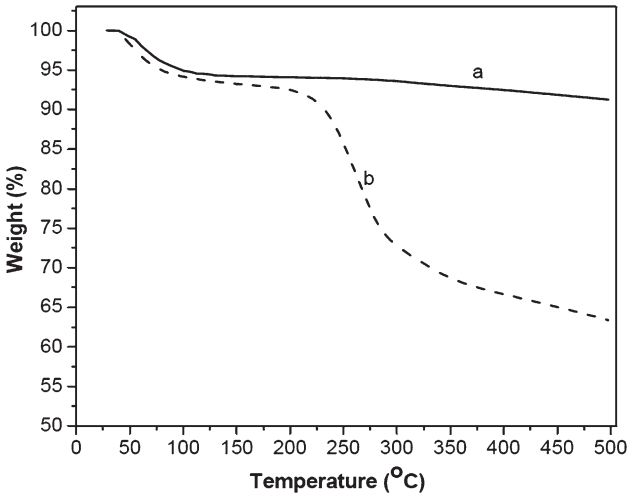

Figure 2. TGA curves of (a) MMT and (b) CMMT.

Compost and Biodegradation

The aerobic compost was prepared using a composition stated in literature.[22,23] The composition of the compost in dry weight is shredded leaves, 11.4%; cow-dung, 40.8%; white bread, 2%; newspaper, 15.8%; saw dust, 7.8%; food waste, 19.2%; urea, 3%. The biodegradation was performed in a perforated glass pot. The biodegradation study was performed in compost with a specimen size of 15 × 15 × 0.1 mm^3 for 100 days. The samples were placed 4 cm beneath the surface of the compost. The temperature was ambient ranging from 20 to 25°C. The moisture content was maintained by spraying water at regular time intervals.

Weight Loss Study

Three samples for each composition were taken out from the compost after a specific time interval. After washing with distilled water thoroughly, samples were dried in a vacuum at 30°C until a constant weight was reached. The average % weight loss was studied by using this formula:

$$\%\ \text{weight loss} = \frac{\{W_o - W_t\} \times 100}{W_o}. \quad (3)$$

Antimicrobial Activity

The antimicrobial activity of PBAT and its nanocomposite films was tested by an inhibition zone method. Food pathogenic bacteria, *Bacillus subtilis* and *Staphylococcus aureus* ware used for testing the antimicrobial activity of the films. For the qualitative measurement of antimicrobial activity, the film samples were punched to make disks (diameter = 11 mm), and the antimicrobial activity was determined using a modified agar diffusion assay (disk test).[24] The plates were examined for possible clear zones after incubation at 37°C for 2 days. The presence of any clear zone that formed around the film disk on the plate medium was recorded as an indication of inhibition against the microbial species.

RESULTS AND DISCUSSION

Characterization of CTAB-Modified MMT

XRD Analysis. The XRD patterns of MMT and CTAB-modified MMT are shown in Figure 1. The diffraction peak at 6.83° is the characteristic peak of MMT attributing to the interlayer distance of 1.29 nm while CTAB-modified MMT (CMMT) shows the usual peak at $2\theta = 4.00°$ corresponding the basal spacing of 2.2 nm. This increase in the basal spacing value belongs to the presence of large hydrophobic groups of CTAB in the clay galleries. It can be said that the MMT has been successfully modified by CTAB where the sodium ion of MMT is replaced by the long chain alkyl ammonium cation of CTAB.

TGA Studies. Figure 2 illustrates the TGA curves of MMT and CMMT. Both the clays show the primary decomposition at the temperature range of 50–100°C attributing to the elimination of water molecules from the clay. The presence of surfactants in the organoclay lowers the surface energy of the inorganic material and converts the hydrophilic to an organophilic one. From the TGA curve it is evident that the thermal stability of MMT is comparatively higher than that of CMMT due to presence of less thermally stable ammonium surfactants in organic-modified MMT.[25]

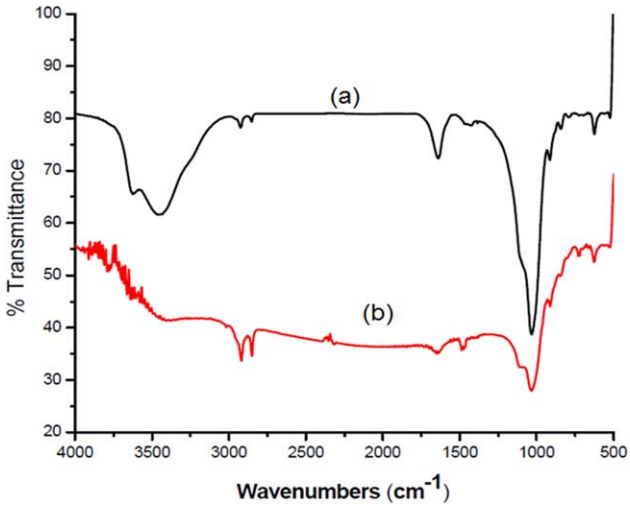

Figure 3. FTIR spectra of (a) MMT and (b) CMMT. [Color figure can be viewed in the online issue, which is available at wileyonlinelibrary.com.]

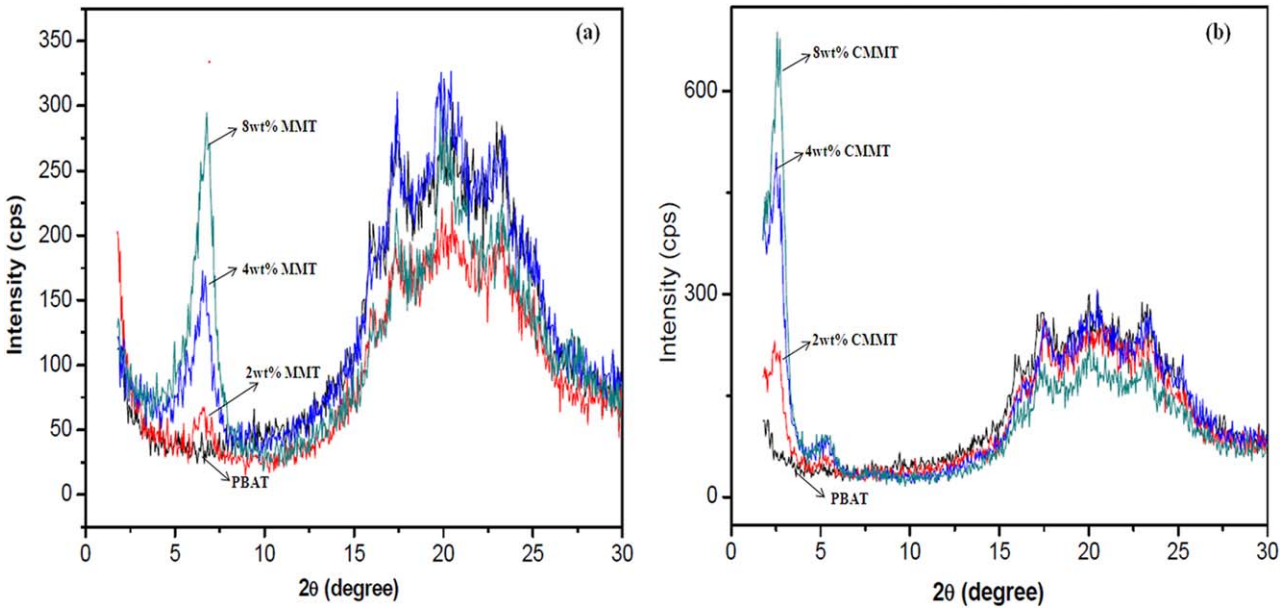

Figure 4. XRD patterns of PBAT and its nanocomposites containing various percentages of (a) MMT and (b) CMMT. [Color figure can be viewed in the online issue, which is available at wileyonlinelibrary.com.]

FTIR Spectroscopy Analysis. Figure 3 shows the FTIR analysis of unmodified MMT and CTAB-modified MMT. From the Figure 3, it is clear that the absorption band at 3454 cm^{-1} of corresponding to —OH stretching vibration of the structural OH groups in MMT is shifted to a lower wave number of 3404 cm^{-1} with modification of the CTAB surfactant. The absorption band of —OH bending vibration of water bonded with hydrated cations of MMT at 1639 cm^{-1} shifted to 1643 cm^{-1} with modification of the CTAB surfactant. The intensity of those bands decreases after modification with the CTAB surfactant due to the replacement of water molecules by surfactant cations.[26] Therefore, it can be concluded that the hydrophilic surface of MMT has been modified to a hydrophobic surface. Conversely, the sharp Si—O stretching band of MMT at 1033 cm^{-1} splits in to a sharp peak of 1035 cm^{-1} with a shoulder around 1110 cm^{-1} with the modification of CTAB surfactant. This significant change in Si—O stretching band of MMT suggests that there is a physical interaction between surface molecules of ammonium bromide in the CTAB $[CH_3(CH_2)_{17}(CH_3)_3N^{\delta+}\ Br^{\delta-}]$ and siloxane $[Si^{\delta+}—O^{\delta-}$ of SiO_4 tetrahedron] in the MMT.[27]

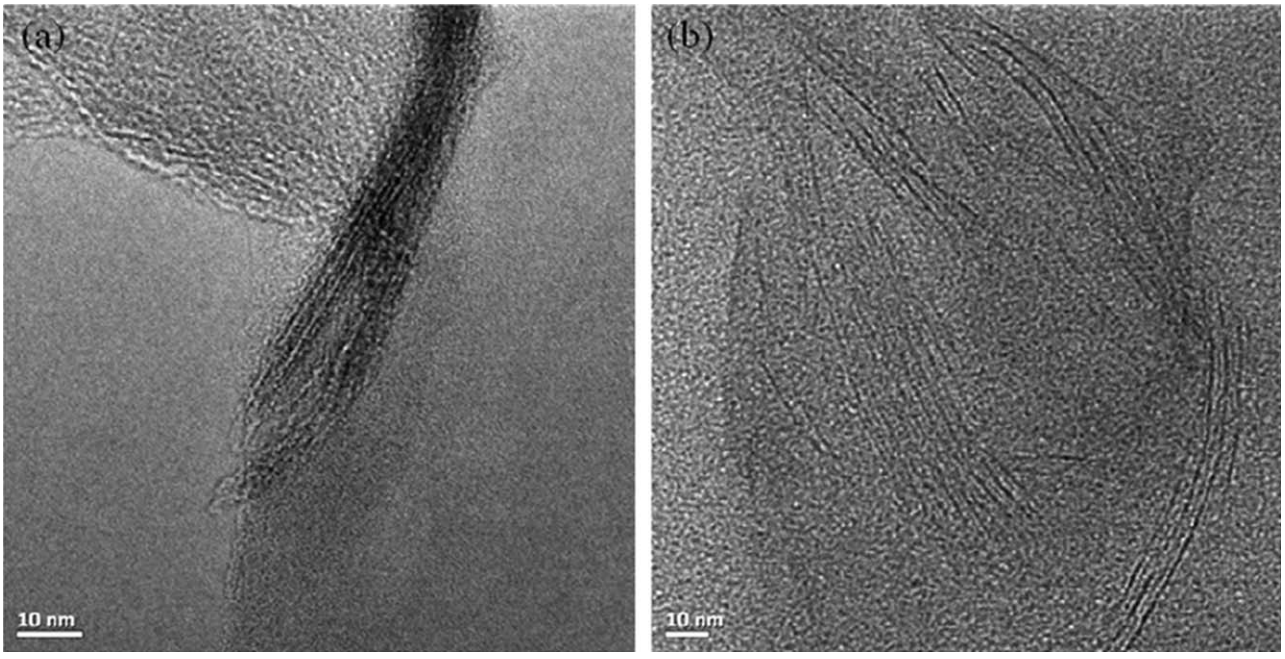

Figure 5. TEM images of PBAT nanocomposite with 4 wt % of (a) MMT and (b) CMMT.

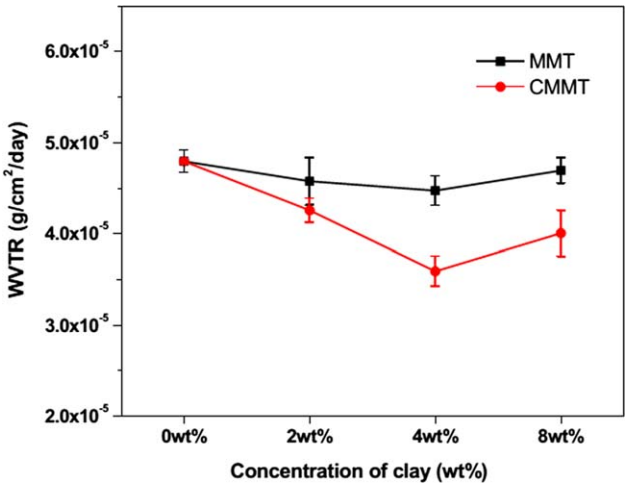

Figure 6. The water vapor transmission rate of PBAT nanocomposites with loading MMT and CMMT. [Color figure can be viewed in the online issue, which is available at wileyonlinelibrary.com.]

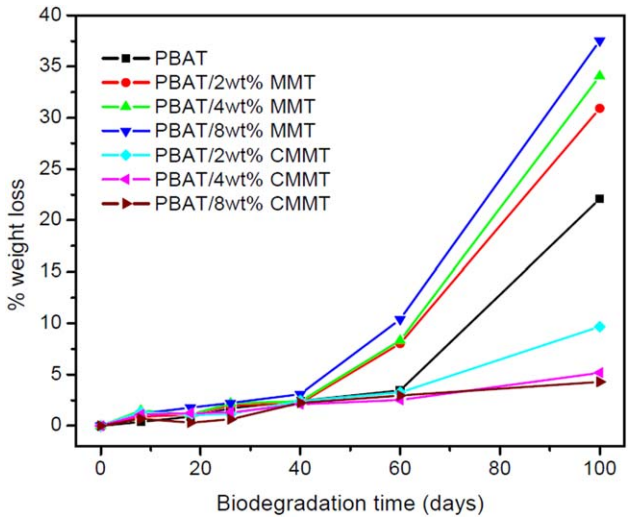

Figure 7. Change in weight loss of the samples with bio-degradation time. [Color figure can be viewed in the online issue, which is available at wileyonlinelibrary.com.]

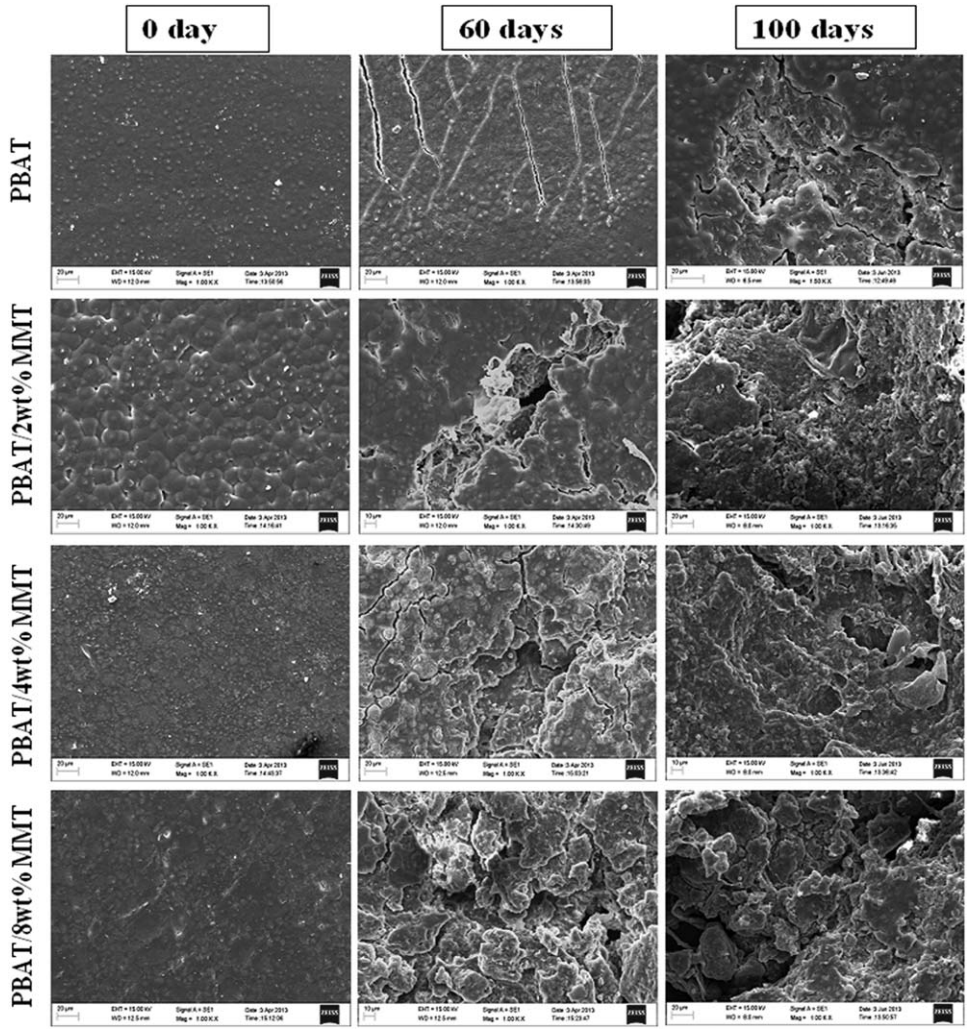

Figure 8. SEM pictures of the biodegraded samples (PBAT and its nanocomposites with 2 wt %, 4 wt %, and 8 wt % MMT) before biodegradation, bio-degradation after 60 days, and biodegradation after 100 days.

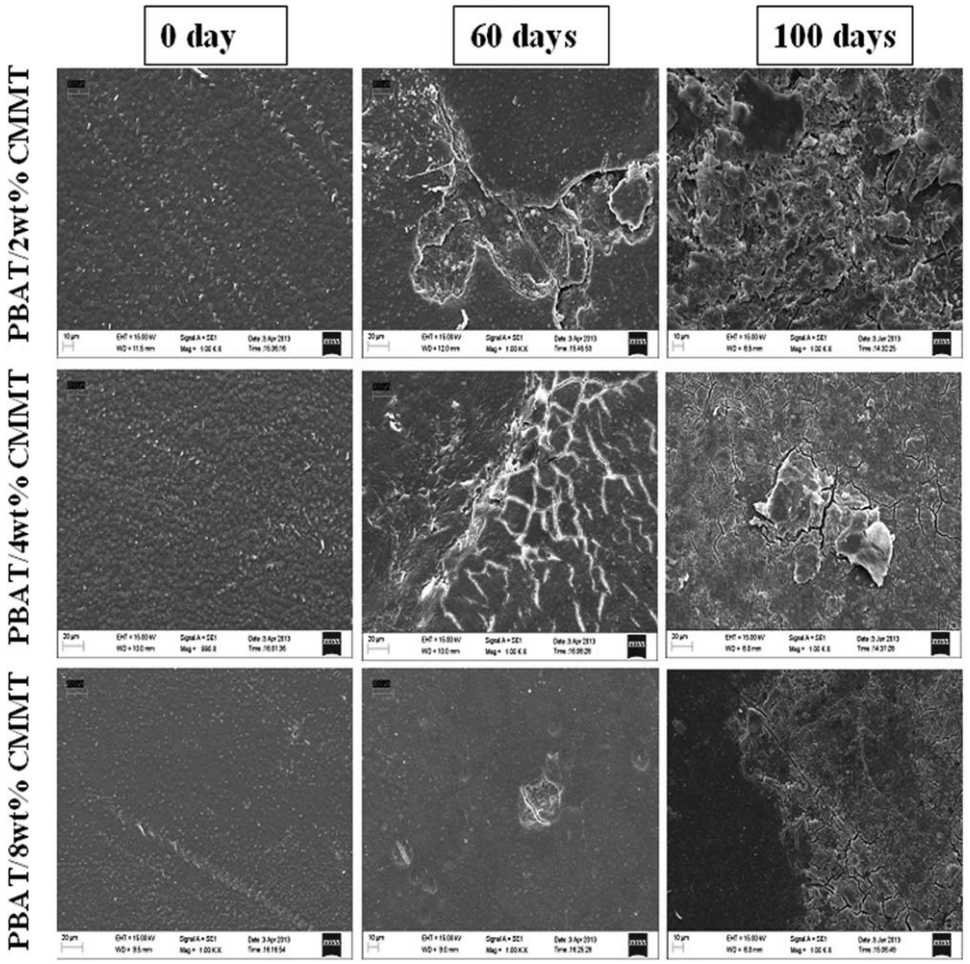

Figure 9. SEM pictures of the biodegraded samples (PBAT/CMMT nanocomposites with 2 wt %, 4 wt %, and 8 wt % CMMT) before biodegradation, biodegradation after 60 days, and biodegradation after 100 days.

Characterization of PBAT/Clay Nanocomposites

XRD Analysis. To scrutinize the nature of the PBAT/clay nanocomposites, XRD analysis has been performed and depicted in the Figure 4. From the XRD results, it can be concluded that the interaction between PBAT polymer and MMT is very low. The diffraction peaks of pristine MMT and PBAT/MMT nanocomposites containing 2 wt %, 4 wt %, and 8 wt % MMT are observed at 6.83°, 6.7°, 6.63°, and 6.76°, respectively, and its corresponding interlayer spacing's are 1.29 nm, 1.32 nm, 1.33 nm, and 1.32 nm, respectively. It is apparent from Figure 4(a) that the characteristic peak for MMT and PBAT/MMT nanocomposites appeared at almost the same 2θ value indicating the very weak or no interaction between the two components present in the nanocomposites which allow them to form immiscible or phase separated microcomposites. Conversely, the diffraction peak of CTAB-modified MMT (CMMT) is obtained at 4.00° corresponding to the interlayer distance of 2.20 nm. For the nanocomposites of PBAT/CMMT containing 2 wt %, 4 wt %, and 8 wt % CMMT, peaks are obtained at 2.59°, 2.65°, and 2.77° with the corresponding interlayer spacing of 3.41, 3.33, and 3.18 nm, respectively. So the conclusion that can be drawn from the results is that the hydrophobic PBAT molecule prefers to interact with organoclay (CMMT) forming the intercalated PBAT/CMMT nanocomposites.

TEM Studies. The dispersion of clay layers in the polymer matrix is observed by TEM and shown in the Figure 5. Figure 5(a,b) shows images of PBAT/4 wt % MMT and PBAT/4 wt % CMMT, respectively. From the TEM image of PBAT/4 wt % MMT [Figure 5(a)], it is clear that MMT layers present as tactoids of agglomerates throughout the polymer matrix due to the very weak interaction between hydrophobic PBAT and hydrophilic MMT. As a result the micro-composite of PBAT/MMT is formed and this observation is in agreement with the XRD results which show very little shifting in the diffraction peak of MMT for PBAT/MMT composites. Conversely, Figure 5(b) established the formation of intercalated nanocomposites of PBAT/CMMT and the interlayer distance is approximately about 3.43 nm, which is close to the interlayer distance of 3.33 nm obtained from XRD analysis. The CMMT with lowered surface energy are more compatible with PBAT and PBAT molecules are able to intercalate within their interlayer space or galleries under well-defined experimental conditions. This is a surface modification which causes the reduction of surface energy of organo-clay layers and matches their surface polarity with polarity of PBAT molecules. So, intercalated nanocomposites are formed in case PBAT/CMMT instead of microcomposite like PBAT/MMT.

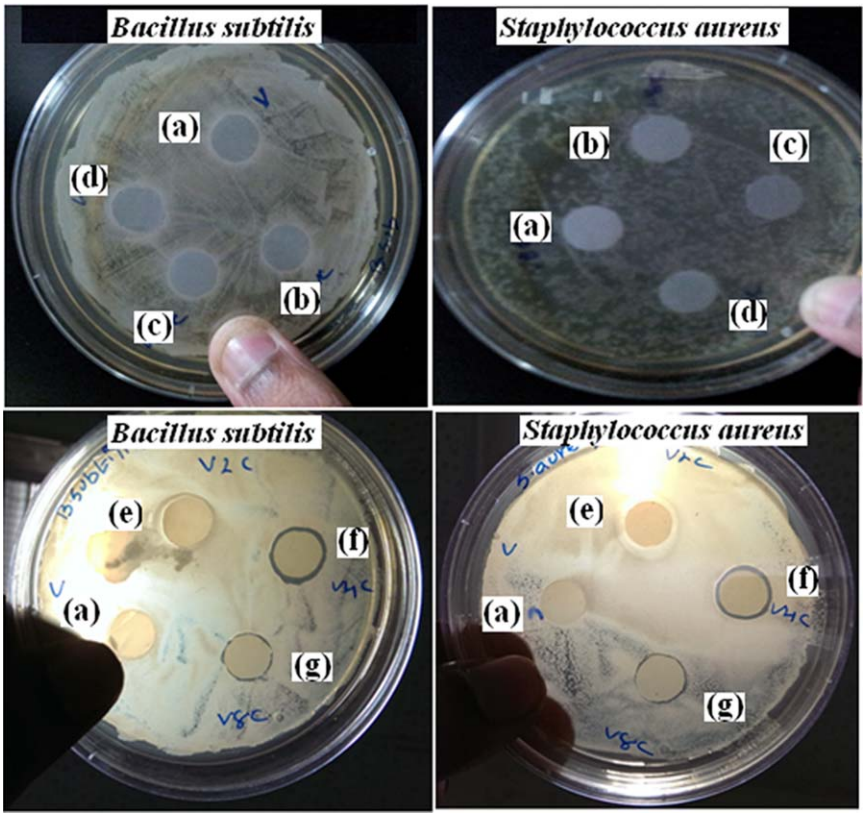

Figure 10. Photograph of antimicrobial test results of (a) PBAT and its nanocomposites with (b) 2 wt % MMT, (c) 4 wt % MMT, (d) 8 wt % MMT, (e) 2 wt % CMMT, (f) 4 wt % CMMT, and (g) 8 wt % CMMT films against *B. subtilis* and *S. aureus*. [Color figure can be viewed in the online issue, which is available at wileyonlinelibrary.com.]

WVTR of Nanocomposite Films

Figure 6 shows the water vapor transmission rate of PBAT and its nanocomposite films. The water vapor transmission rate of PBAT film is obtained at 4.8×10^{-5} g/cm^2 per day and it decreases for both the MMT and CMMT nanocomposites. The decreasing trend in water vapor transmission rate is more dominant for CMMT as CMMT and PBAT form a uniform dispersion where adequate interaction gives rise to intercalated nanocomposites. With the addition of 2 wt %, 4 wt %, and 8 wt % MMT in PBAT film, the water vapor transmission rate (WVTR) of nanocomposites is decreased by 4.6%, 6.87%, and 2.08%, respectively, whereas the water vapor transmission rate of PBAT films is decreased by 11.25%, 25.21%, and 16.45% with the addition of 2 wt %, 4 wt %, and 8 wt % CMMT, respectively. So it is quite clear that the water vapor transmission rate of PBAT film is reduced marginally in the presence of MMT due to very weak interactions present between the polymer and MMT layers. Conversely, the impermeable CMMT clay layers in the PBAT matrix increases the effective diffusion path length for moisture and increases the water vapor barrier property of the nanocomposite film.[4,28] For PBAT/CMMT nanocomposite film, the decrease in WVTR is more prominent in the case of 4 wt % CMMT attributing to the tortuous path for water vapor diffusion which in turn plays the important role from an application viewpoint. It is predictable that after a certain amount of clay impregnation into the polymer matrix, it does not improve the WVTR[29,30] as it is clear from the figure and may be said that the greater amount of clay in the polymer matrix undergoes agglomeration which prevents the film to show the satisfactory amount of WVTR.

Biodegradation of Nanocomposite Films

Weight loss curve of PBAT and its nanocomposite films during aerobic biodegradation process in compost is shown in Figure 7. It is clearly noticeable from the figure that the greater the incubation time, the higher the weight loss of PBAT film and the weight loss of 3.45 wt % and 22.09 wt % are measured for the pure PBAT film after 60 and 100 days, respectively. To fully visualize the effect of MMT, we have taken the SEM images of each recipe made of PBAT and MMT. It is quite understandable that MMT being a hydrophilic clay should have the significant effect on the biodegradation rate of PBAT/MMT nanocomposite films and it is evident that with an increasing MMT concentration, the rate of biodegradation of PBAT film increases, as witnessed from the SEM images given in the Figure 8. Among the samples, PBAT/8 wt % MMT film shows highest biodegradation rate which is about 10.05 wt % and 37.54 wt % after 60 days and 100 days, respectively.

From the SEM images it can be concluded that the incorporation of MMT in the PBAT matrix erodes the surface of PBAT owing to its higher biodegradation rate. The holes and cracks present on the surface of pure PBAT becomes more intense as the concentration of MMT increases and reaches to the

maximum in the case of PBAT/8 wt % MMT attributing the hydrophilic nature of unmodified nanoclay.[31] Conversely, the rate of biodegradation of PBAT film decreases with incorporation of organically modified nanoclays. From the Figure 7 it is calculated that after 100 days, the weight loss of PBAT film is about 9.67 wt %, 5.18 wt %, and 4.29 wt % with the incorporation of 2 wt %, 4 wt %, and 8 wt % CTAB-modified clay, respectively.

To investigate the surface morphology, the SEM images of PBAT/CMMT nanocomposites films are taken and given in the Figure 9. From the Figure 9, it is quite comprehensible that with increasing the concentration of CMMT in the PBAT matrix the rate of biodegradation of the films decreases and as a result of this the comparatively smooth surface with less cracks and holes is obtained in the case of PBAT/8 wt % CMMT film among all the compositions. In the case of hydrophobic organo-modified clay, the homogeneous dispersion of silicate layers in the polymer matrix obstructs the enzymes to penetrate through the composite films[2] or hinder the water diffusion through it as the CMMT increases the effective diffusion path length or the tortuous paths of PBAT which is also responsible for lowering of WVTR.

Antimicrobial Activity of Nanocomposite Films

As these types of nanocomposite films are the emerging candidate in the field of packaging applications and in this context, antimicrobial property must be one of the characteristic features of these type polymer nanocomposites. The antimicrobial activity of the films by the disk method against *B. subtilis* and *S. aureus* is shown in the Figure 10. As evident from the images that the PBAT and PBAT/MMT nanocomposite films do not show clear microbial inhibition zones, whereas CTAB-modified MMT incorporated PBAT nanocomposite films exhibits distinctive microbial inhibition zones in the disk method for both the microorganisms. Zones of inhibition diameter of PBAT/CMMT nanocomposites are 11.2, 13.7, 12.0 mm against *B. subtilis* and 11.1, 13.5, 11.5 mm against *S. aureus* with loading 2 wt %, 4 wt %, and 8 wt % CMMT, respectively. Therefore, PBAT/4 wt % CMMT nanocomposite film shows efficient antimicrobial properties against both microorganisms than the others. In lieu of this context, it can be said that the presence of long chain hydrophobic alkyl and cationic charge of a quaternary ammonium group in CMMT can strongly inhibit the growth of microbes.[18]

CONCLUSIONS

A comparative study between MMT and CMMT-based nanocomposites has been described in this article. We have successfully modified the MMT and prepared the PBAT/clay nanocomposites via solution intercalation process. Among the two types of nanocomposites, PBAT/CMMT shows the greater degree of property enhancement like water vapor transmission rate, and antimicrobial property due to the intercalated morphology and presence of quaternary ammonium cation in the CMMT of nanocomposite. Besides this, the same offers the better resistance towards degradation in the presence of different microorganisms in compost. As the PBAT/CMMT nanocomposites offer greater resistance to the colonization of gram-positive bacteria, for example, *B. subtilis* and *S. aureus* owing to the presence of quaternary ammonium cation, so it is unsurprising that PBAT/CMMT nanocomposites shows the lower degree of biodegradation.

ACKNOWLEDGMENTS

D. Mondal likes to thank the Council of Scientific & Industrial Research (CSIR), Govt. of India for providing senior Research Fellowship. B. Bhowmick likes to thank the Centre for Nanoscience and Nanotechnology, University of Calcutta. Md. M. R. Mollick likes to thank Department of Science & Technology (DST), Govt. of India for his fellowship, and D. Maity likes to thank the University Grant Commission, Govt. of India for her fellowship.

REFERENCES

1. Chang, J. H.; An, Y. U.; Cho, D.; Giannelis, E. P. *Polymer* **2003**, *44*, 3715.
2. Ludueña, L. N.; Vázquez, A.; Alvarez, V. A. *J. Appl. Polym. Sci.* **2013**, *128*, 2648.
3. Almasi, H.; Ghanbarzadeh, B.; Entezami, A. A. *Int. J. Biol. Macromol.* **2010**, *46*, 1.
4. Mondal, D.; Bhowmick, B.; Mollick, M. R. M.; Maity, D.; Mukhopadhyay, A.; Rana, D.; Chattopadhyay, D. *Carbohydr. Polym.* **2013**, *96*, 57.
5. Rodríguez, F. J.; Coloma, A.; Galotto, M. J.; Guarda, A.; Bruna, J. E. *Polym. Degrad. Stab.* **2012**, *97*, 1996.
6. de la Orden, M. U.; Pascual, D.; Antelo, A.; Arranz-Andrés, J.; Lorenzo, V.; Martínez Urreaga, *J. Polym. Degrad. Stab.* **2013**, *98*, 1110.
7. Ray, S. S.; Maiti, P.; Okamoto, M.; Yamada, K.; Ueda, K. *Macromolecules* **2002**, *35*, 3104.
8. Singh, N. K.; Purkayastha, B. D.; Roy, J. K.; Banik, R. M.; Yashpal, M.; Singh, G.; Malik, S.; Maiti, P. *ACS Appl. Mater. Interfaces* **2010**, *2*, 69.
9. Sancha, R.; Bajpai, J.; Bajpai, A. K. *Polym. Comp.* **2011**, *32*, 537.
10. Phua, Y. J.; Lau, N. S.; Sudesh, K.; Chow, W. S.; Mohd Ishak, Z. A. *Polym. Degrad. Stab.* **2012**, *97*, 1345.
11. Ray, S. S.; Bousmina, M. *Prog. Mater. Sci.* **2005**, *50*, 962.
12. He, H.; Ma, Y.; Zhu, J.; Yuan, P.; Qing, Y. *Appl. Clay Sci.* **2010**, *48*, 67.
13. Witt, U.; Einig, T.; Yamamoto, M.; Kleeberg, I.; Deckwer, W.-D.; Müller, R.-*J. Chemosphere* **2001**, *44*, 289.
14. Someya, Y.; Sugahara, Y.; Shibata, M. *J. Appl. Polym. Sci.* **2005**, *95*, 386.
15. Chen, J.-H.; Chen, C.-C.; Yang, M.-C. *J. Polym. Res.* **2011**, *18*, 2151.
16. Mohanty, S.; Nayak, S. K. *Polym. Comp.* **2010**, *31*, 1194.
17. Rhim, J.-W.; Hong, S.-I.; Park, H.-M.; Ng, P. K. W. *J. Agric. Food Chem.* **2006**, *54*, 5814.
18. Rhim, J.-W.; Hong, S.-I.; Ha, C.-S. *LWT Food Sci. Technol.* **2009**, *42*, 612.
19. Standard test methods for water vapor transmission of material—E-96-00, In Annual Book of ASTM Standards; ASTM International: 100 Barr Harbor Drive, West Conshohocken, PA 19428-2959, 2010; DOI: 10.1520/E0096_E0096M-12.

20. Cyras, P. V.; Manfredi, B. L.; That, T. T. M.; Vázquez, A. *Brazilian Arch. Biol. Technol.* **2011**, *54*, 1223.
21. Mohd Amin, M. C. I.; Abadi, G. A.; Ahmad, N.; Katas, H.; Jamal, J. A. *Sains Malaysiana* **2012**, *41*, 561.
22. Singh, R. P.; Pandey, J. K.; Rutot, D.; Degée, P.; Dubois, P. *Carbohydr. Res.* **2003**, *338*, 1759.
23. Maiti, S.; Ray, D.; Mitra, D.; Misra, M. *J. Appl. Polym. Sci.* **2012**, *123*, 2952.
24. Mollick, M. M. R.; Bhowmick, B.; Maity, D.; Mondal, D.; Bain, M. K.; Bankura, K.; Sarkar, J.; Rana, D.; Acharya, K.; Chattopadhyay, D. *Int. J. Green Nanotechnol.* **2012**, *4*, 230.
25. Mallakpour, S.; Dinari, M. *Appl. Clay Sci.* **2011**, *51*, 353.
26. Wang, L.; Wang, A. *J. Hazard. Mater.* **2008**, *160*, 173.
27. Karaca, S.; Gürses, A.; Korucu, M. E. *J. Chem.* **2013**, 2013, 274838 (10 pp).
28. Cussler, E. L.; Hughes, S. E.; Ward, W. J., III; Aris, R. J. *J. Membr. Sci.* **1998**, *38*, 161.
29. Park, H.-M.; Li, X.; Jin, C.-Z.; Park, C.-Y.; Cho, W.-J.; Ha, C.-S. *Macromol. Mater. Eng.* **2002**, *287*, 553.
30. Chiou, B.-S.; Wood, D.; Yee, E.; Imam, S. H.; Glenn, G. M.; Orts, W. *J. Polym. Eng. Sci.* **2007**, *47*, 1898.
31. Someya, Y.; Kondo, N.; Shibata, M. *J. Appl. Polym. Sci.* **2007**, *106*, 730.